Published online 4 June 2012 *Nucleic Acids Research, 2012, Vol. 40, No. 16* ***8119–8128***
doi:10.1093/nar/gks512

High-resolution structures of two complexes between thrombin and thrombin-binding aptamer shed light on the role of cations in the aptamer inhibitory activity

Irene Russo Krauss[1], Antonello Merlino[1,2], Antonio Randazzo[3], Ettore Novellino[3], Lelio Mazzarella[1,2] and Filomena Sica[1,2,*]

[1]Dipartimento di Scienze Chimiche, Università di Napoli Federico II, Via Cintia, I-80126 Napoli, Italia [2]Istituto di Biostrutture e Bioimmagini, C.N.R., Via Mezzocannone 16, I-80134 Napoli, Italia and [3]Dipartimento di Chimica Farmaceutica e Tossicologica, Università di Napoli Federico II, Via D. Montesano 49, I-80131 Napoli, Italia

Received January 31, 2012; Revised May 8, 2012; Accepted May 9, 2012

ABSTRACT

The G-quadruplex architecture is a peculiar structure adopted by guanine-rich oligonucleotidic sequences, and, in particular, by several aptamers, including the thrombin-binding aptamer (TBA) that has the highest inhibitory activity against human α-thrombin. A crucial role in determining structure, stability and biological properties of G-quadruplexes is played by ions. In the case of TBA, K^+ ions cause an enhancement of the aptamer clotting inhibitory activity. A detailed picture of the interactions of TBA with the protein and with the ions is still lacking, despite the importance of this aptamer in biomedical field for detection and inhibition of α-thrombin. Here, we fill this gap by presenting a high-resolution crystallographic structural characterization of the thrombin–TBA complex formed in the presence of Na^+ or K^+ and a circular dichroism study of the structural stability of the aptamer both free and complexed with α-thrombin, in the presence of the two ionic species. The results indicate that the different effects exerted by Na^+ and K^+ on the inhibitory activity of TBA are related to a subtle perturbation of a few key interactions at the protein–aptamer interface. The present data, in combination with those previously obtained on the complex between α-thrombin and a modified aptamer, may allow the design of new TBA variants with a pharmacological performance enhancement.

INTRODUCTION

It has been known for a long time that guanine-rich oligonucleotidic sequences can arrange in a quadruple helix structure, named G-quadruplex (1). The main component of G-quadruplexes is the G-tetrad or G-quartet, a planar arrangement of four guanine bases associated through a cyclic array of Hoogsteen-like hydrogen bonds, in which each guanine base both accepts and donates two hydrogen bonds (1). Stacked G-quartets with their O6 atoms line a central cavity with a strong negative electrostatic potential, where cations are well accommodated (2). These cations play an important role in the formation, topology and stability of G-quadruplexes (3).

The G-quadruplex architecture is adopted by several aptamers. These are DNA- or RNA-based oligonucleotides selected from large combinatorial pools of sequences for their capacity to efficiently recognize targets (4,5). The best known aptamer is a DNA 15-mer whose sequence is 5′-GGTTGGTGTGGTTGG-3′, which is named thrombin-binding aptamer (TBA) (4), because of its inhibitory properties against human α-thrombin, a pharmacologically relevant protein that plays a pivotal role in hemostasis (6). The structure of TBA was solved by nuclear magnetic resonance (NMR) spectroscopy in the 90s (7,8): it folds as an anti-parallel chair-like G-quadruplex structure, with two G-tetrads surrounded by a TGT loop on one side and two TT loops on the opposite side. From the first discovery of TBA, this molecule and its variants have been extensively studied in terms of structure (by using NMR and circular dichroism (CD)), stability and α-thrombin affinity (9–20). It has been shown that modifications of the original TBA sequence and/or of cation composition of the buffer result in changed biophysical properties and anticoagulant activity that were in some cases attributed to different folding topologies and molecularity (9,21–25). Furthermore, TBA has been studied for its potentiality in therapeutic (26–29) and diagnostic fields (30–32), thanks to its ability to strongly and specifically recognize α-thrombin.

The details of the interaction between TBA and thrombin are still lacking, despite the great importance

*To whom correspondence should be addressed. Tel: +39 081 674479; Fax: +39 081 674090; Email: filomena.sica@unina.it

of TBA in biomedical field for both detection and inhibition of α-thrombin. Indeed, thrombin–TBA complex structure was solved by X-ray crystallography at 2.9 Å resolution (33). However, diffraction data were of low quality and in a first model of the complex (PDB code 1HAP), the TBA molecule rebuilt in electron density maps has a different topology with respect to the NMR structure (7,8): in the latter TGT loop spans a wide groove of the quadruplex helix and TT loops span the two narrow grooves, whereas the opposite is observed in the crystallographic structure. A second model of the complex was built using slightly higher resolution diffraction data (2.8 Å resolution) and the coordinates of the NMR structure of TBA in the fitting procedure (PDB code 1HAO) (34). Besides the difference in topology of TBA, in the two X-ray models, the orientation of the aptamer with respect to thrombin also differs by a rotation of 180° about an axis parallel to the two G-quartet planes. In particular, TBA interacts with the fibrinogen-binding site of α-thrombin (exosite I) by the TGT loop in 1HAP, and by the TT loops in 1HAO. A later and more exhaustive examination of the diffraction data suggested that the NMR-derived model (1HAO) was likely to be the correct one (35). However, the low quality of electron density in the region of TBA loops did not provide an unambiguous description of the thrombin–TBA-binding interactions; moreover, 1HAP is still often used as a model for the design of new TBA-modified aptamers (12,14).

As recalled earlier, ions play a crucial role in determining the structure, stability and biological properties of G-quadruplexes. The ions are supposed to favour the thrombin/aptamer interaction by stabilizing the folding of the aptamer. In particular, the presence of potassium ions gives more stable quadruplexes than other univalent cations and enhances the thrombin-inhibiting effect of the aptamer (36,37). At the same time, α-thrombin is able to act as a molecular chaperone on the aptamer, inducing and/or stabilizing TBA quadruplex fold, regardless the presence of cations (13,38).

We have performed a detailed X-ray diffraction study of the protein–aptamer complex formed in the presence of Na^+ (thrombin–TBA–Na) at 1.80 Å resolution or K^+ (thrombin–TBA–K) at 2.05 Å resolution. Stability of the aptamer structure, free and in complex with α-thrombin in the presence of the two ionic species was also monitored by CD. Together with the previously published data on the high-resolution crystal structure of the complex between α-thrombin and the variant mTBA (39), the present results definitively qualify the two TT loops as the aptamer recognition motif of the thrombin exosite I that is responsible for the elevated stability of the complex. Moreover, the well-defined electron density in the region of the aptamer loops provides unambiguous details on the protein–aptamer interface. The data here presented also suggest that the different ability of Na^+ and K^+ in reducing the inhibitory activity of TBA is related to subtle structural variations involving key protein–aptamer interactions rather than to the effect of ions on the stability of the TBA structure.

MATERIALS AND METHODS

Sample preparation, crystallization and data collection

The human D-Phe-Pro-Arg-chloromethylketone (PPACK)–inhibited α-thrombin was purchased from Haemtech. Two different samples of α-thrombin were prepared, changing the initial buffer to MCl 0.75 M, where M is either Na^+ or K^+, using Centricon mini-concentrator and a refrigerated centrifuge. TBA was purchased from Genosys. Stock solutions of the aptamer, at a concentration of 2 mM, were prepared dissolving the lyophilized oligonucleotide in 10 mM sodium (TBA–Na) or potassium (TBA–K) phosphate buffer pH 7.1 Nucleotide samples were heated for 10 min at 85°C and then slowly cooled down and stored at 4°C overnight. The complexes with thrombin were prepared, as previously described (40), by placing a 2-fold molar excess of aptamer on a frozen sample of inhibited thrombin and leaving the sample at 4°C for 3 h. Then, the samples were diluted and the buffer changed to 0.025 M M-phosphate pH 7.1 and 0.1 M MCl, where M was either Na^+ or K^+, for thrombin–TBA–Na and thrombin–TBA–K, respectively. The thrombin–TBA complexes were extensively washed to take off the excess of aptamer and finally concentrated to about 8 mg/ml using Centricon mini-concentrator and a refrigerated centrifuge.

Crystallization conditions were identified after an extensive screening performed using commercial kits and an automated crystallization system. The starting crystallization solution contained 20% wt/vol polyethylene glycol 8000, 0.2 M zinc acetate and 0.1 M sodium cacodilate pH 6.5. Using the sitting drop vapour diffusion method, the optimized conditions were found to be very similar for both complexes. The best diffracting crystals grew from drops of 1 µl, obtained by mixing equal volumes of complex solution (8 mg/ml) and reservoir solution (10–15% wt/vol polyethylene glycol 8000, 0.05 M zinc acetate and 0.1 M sodium cacodilate pH 7.4). Diffraction data from both complexes were collected in-house on a Saturn944 CCD detector. The X-ray radiation used was Cu-Kα radiation from a Rigaku Micromax 007 HF generator. After the addition of 25% glycerol to the harvesting solution, crystals were flash-cooled at 100 K in supercooled N_2 gas produced by an Oxford Cryosystem and maintained at 100 K during the data collection. All the data were indexed, processed and scaled with HKL2000 (41). Crystals of both thrombin–TBA complexes have a different symmetry from those previously studied (1HAP and 1HAO). They belong to the triclinic space group P1 and diffract up to 1.80 and 2.05 Å resolution for thrombin–TBA–Na and thrombin–TBA–K, respectively. Matthews' coefficient calculations suggested the presence of a 1:1 complex in the asymmetric unit. Detailed statistics on data collection are reported in Supplementary Table S1.

Structure determination and refinement

The structure of thrombin–TBA–K was solved by the molecular replacement method using the program Phaser (42) and coordinates of both inhibited thrombin (derived from

the structure of its complex with mTBA, PDB code 3QLP) and TBA (derived from the structure of the complex with thrombin, PDB code 1HAO) as search models. To avoid bias, PPACK, ions and water molecules were removed from the model. A clear solution was obtained with a *Z*-score of 12.5 and a log-likelihood gain (LLG) of 1206. The structure of thrombin–TBA–Na was obtained starting from thrombin–TBA–K model: several cycles of rigid body refinement with CNS program (43) were performed in the resolution range 10.0–3.0 Å, treating TBA and thrombin as distinct rigid groups. The *R* factor for the model thus obtained was 0.360. The two structures were then refined through several cycles of coordinate and *B* factor minimization with CNS (43). Each run was alternated with manual model building using the program O (44). Analysis of difference Fourier maps, calculated at various stages of refinement, allowed the fitting of PPACK in the active site, the positioning of several ions and water molecules, and the identification of a glycosylation site on Asn60G of the thrombin heavy chain. After including of low-resolution data and bulk solvent correction, the crystallographic *R* factor and R_{free} for the thrombin–TBA–Na final model, in the resolution range 50.0–1.80 Å, were 0.175 and 0.225, respectively, whereas for the thrombin–TBA–K final model in the resolution range 50.0–2.05 Å were 0.174 and 0.226, respectively. In thrombin–TBA–K, the potassium ion was unambiguously identified from anomalous difference Fourier peaks. The programs used in locating anomalous scatterers were from the CCP4 suite (45). TRUNCATE was used to calculate the amplitude of structure factors and anomalous difference from the measured intensities, PHASER to find anomalous scatterers in the refined model and FFT to generate anomalous difference Fourier maps. At the end of refinement, the geometry of all the protein structures was monitored using PROCHECK (46) and WHATCHECK (47). A full list of refinement statistics is reported in Supplementary Table S2. All residue fall in 'allowed' regions of the Ramachandran map with the exception of two residues of a flexible loop of thrombin–TBA–K.

The drawings were prepared with Pymol (http://pymol.org). The coordinates of the structures have been deposited in the Protein Data Bank (Codes 4DIH and 4DII, for thrombin–TBA–Na and thrombin–TBA–K, respectively).

Structural analysis of thrombin–aptamers complexes

Features of the thrombin–TBA interface in the two complexes, including buried surface area, number and types of residues at the interface, and gap volume index, were calculated using the Protein–Protein Interaction Server (http://www.bioinformatics.sussex.ac.uk/protorp/). The shape complementarity score, Sc, as defined by Lawrence and Colman (48), was calculated using the CCP4 package (45), opportunely modified to include nucleic acid parameters. Packing interactions between the aptamer and thrombin molecules were found using the Contact routine of CCP4 package (45) and by visual inspection of the structure with O program (44).

CD measurements

CD spectra were recorded at 10°C using a Jasco J-710 spectropolarimeter equipped with a Peltier thermostatic cell holder (Model PTC-348WI). CD measurements in the 200–350 nm range for the aptamer free and complexed with α-thrombin were performed using a 0.1 cm path length cell and aptamer or protein concentration 7.0 μM in 0.025 M M-phosphate buffer pH 7.1 and 0.1 M MCl, where M was either Na^+ or K^+. Before measurements, the samples were pre-equilibrated at 10°C for 5 min and the instrument was calibrated with an aqueous solution of d-10-(+)-camphorsulfonic acid at 290 nm. Thermal unfolding curves were recorded in the 10–90°C range, in 1°C steps with 0.5 min equilibration time between readings, at heating rate 1°C/min. No differences in melting transitions were observed when the scan rate was increased to 5°C/min. The temperature/wavelength mode was used: CD signal was followed at 295 nm and the whole spectrum was recorded in the 200–350 nm range every 5°C. Melting temperatures for TBA were calculated from the first derivative of the molar ellipticity change vs. temperature.

RESULTS

CD measurements

The effect of sodium or potassium buffers and/or of α-thrombin on thermal stability of TBA tertiary structure has been tested by means of CD. TBA folds in the expected antiparallel quadruplex structure when either sodium or potassium ions are added to a solution of the aptamer at 10°C. This is clearly shown by CD spectra that present the typical maximum at 295 nm, the two additional positive peaks at 210 and 250 nm and the minimum at 270 nm (Figure 1A and B, blue lines). These spectral features are fully recovered after annealing at 90°C, indicating that the presence of the ions is sufficient to induce the correct folding of the aptamer (Figure 1A and B, red lines).

The thermal stability of TBA was investigated in the 10–90°C range following the CD signal at 295 nm and recording the whole CD spectrum every 5°C. The melting temperatures of TBA in the presence of Na^+ (Figure 2A, dashed line) and K^+ (Figure 2B, dashed line) are 24 and 53°C, respectively, in good agreement with those reported in literature (12,13). When α-thrombin is added to the solution in an equimolar ratio to TBA, the melting curves indicate a considerable increase in the thermal stability of the quadruplex structure. The melting temperature of TBA rises up to 58°C (Figure 2A, bold line) and up to 70°C in the presence of Na^+ and K^+ (Figure 2B, bold line), respectively. To investigate the stability of the complexes at the temperature used for testing inhibitory activity of the aptamer (36,37), CD spectra of TBA were recorded in the presence of thrombin and Na^+ or K^+ for 5 h every 5 min at 37°C. No appreciable variation of the CD signals in the quadruplex region has been observed for both complexes (data not shown).

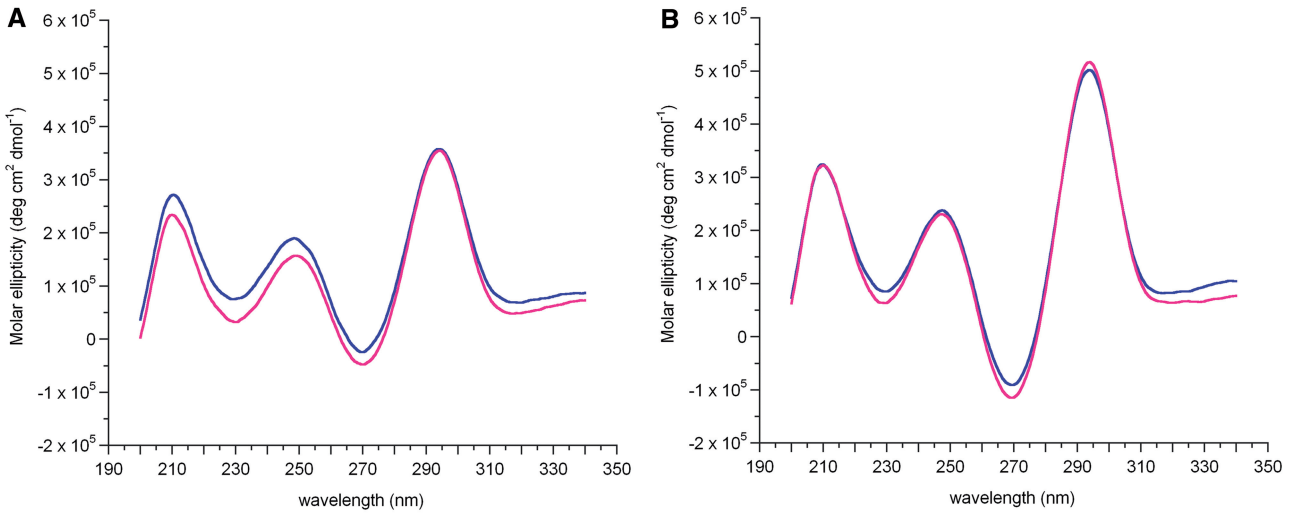

Figure 1. CD spectra of 7 μM TBA in 25 mM M-phosphate buffer pH 7.1 and 0.1 M MCl, where M is either Na^+ (**A**) and K^+ (**B**) at 10°C before (blue line) and after (red line) annealing at 90°C.

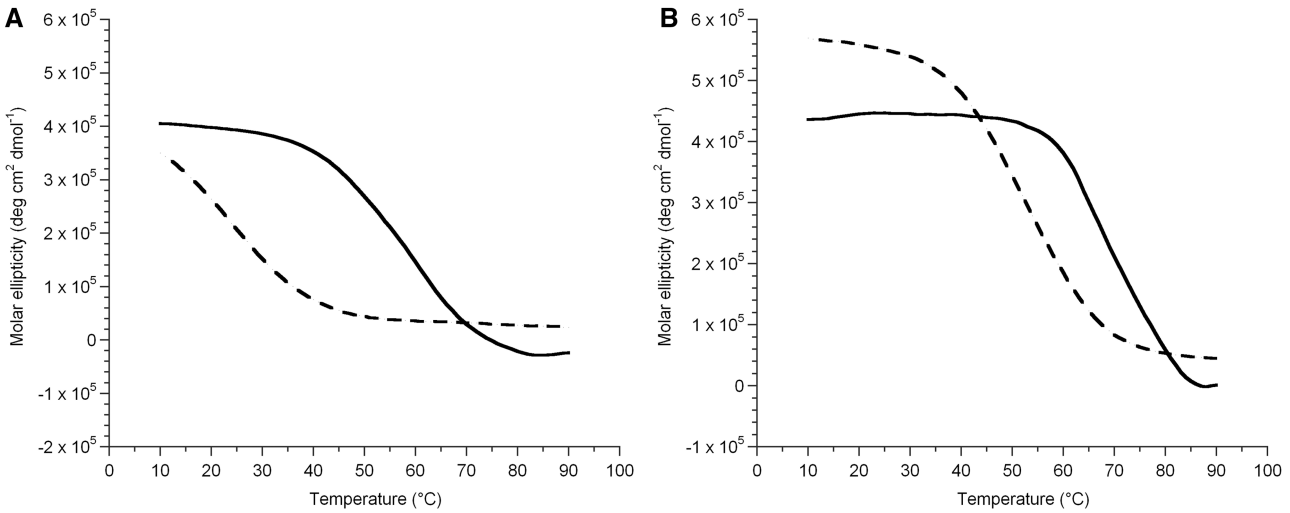

Figure 2. Thermal denaturation of TBA as followed by CD spectroscopy at 295 nm, in the absence (dashed line) and in the presence (bold line) of an equimolar amount of thrombin at a heating rate of 1°C/min. Measurements were carried out in 25 mM M-phosphate buffer pH 7.1 and 0.1 M MCl, where M is either Na^+ (**A**) and K^+ (**B**), using a 7 μM aptamer concentration.

Overall crystal structures

Good quality crystals of thrombin–TBA complex in the presence of Na^+ (thrombin–TBA–Na) and in the presence of K^+ (thrombin–TBA–K) were grown and used for the X-ray diffraction analysis. The former complex was solved at 1.80 Å and refined to R factor/R_{free} values of 0.175/0.225, whereas the latter was solved at 2.05 Å and refined to 0.174/0.226. The crystals are isomorphous and belong to the triclinic space group P1. Detailed statistics of the refinement are reported in Supplementary Table S2.

In both complexes, the heavy chain (residues 16–246) and the light chain (residues 1B-14 K) of the thrombin molecule are well defined, with the exception of the γ-autolysis loop (residues 148–150) of the heavy chain. The electron density maps corresponding to TBA are also clear and continuous, with the only exception of the Thy9 base of thrombin–TBA–Na. In the presence of sodium or potassium ions, TBA folds as a chair-like quadruplex with a core that is formed by two stacked G-quartets and covered by the TGT loop on one side and the two TT loops on the opposite side. The aptamer topology is in full agreement with the NMR model (7,8); in particular, TT loops span the two narrow grooves, whereas the TGT loop spans a wide groove.

Despite the differences in the crystal packing and symmetry, the present crystal structures and those previously published for thrombin–TBA (1HAO) (33,34) and for thrombin–mTBA (3QLP) (39,40) complexes present two invariant features: (a) the asymmetric unit contains one thrombin and one aptamer molecule and (b) apart

from the 1HAO structure, the most extended interface between the two molecules is composed by the thrombin exosite I and the two TT loops of the aptamer (Figure 3).

In all crystal forms, the protein also interacts with a second symmetry-related aptamer; the regions involved in this additional interaction surface change from one structure to the other and the overall area is significantly less extended with respect to the invariant interface. The only exception is represented by the low-resolution structure 1HAO where the two interfaces are comparable. In thrombin–TBA–K and thrombin–TBA–Na, whose crystals are isomorphous, one residue of the exosite II only marginally contacts the TGT loop of TBA. Moreover, in the thrombin–mTBA crystal structure, the additional interaction surface does not involve at all residues from the exosite II region. Altogether, these features strongly indicate that this secondary interface is the result of the packing optimization rather than of a specific recognition pattern between α-thrombin and the aptamers and further support the conclusion that the surviving complexes in solution should have the 1:1 stoichiometry displayed in the solid state (39,40).

Coordination of the alkaline ions

Examination of difference Fourier maps clearly shows the presence of a strong electron density peak, positioned between the two G-quartets, marking the position of the alkaline ion in the two crystal structures. Furthermore, the anomalous difference Fourier map definitely shows that in the case of thrombin–TBA–K, the electron density peak represents a bound potassium ion. It is interesting to note that in the case of thrombin–TBA–Na, the residual electron density resembles that of a prolated ellipsoid (Figure 4A), whereas in the case of thrombin–TBA–K, its shape is nearly spherical (Figure 4B). As K^+ is unequivocally identified from its anomalous signal (Supplementary Figure S1), the different shape of the two peaks can be linked to the different ionic radius of the two ions. In thrombin–TBA–K the potassium ion, centred in the electron density peak, is in a proper position to make coordination bonds to the four purine O6 atoms of both quartets according to a distorted anti-prism geometry. The observed coordination bonds range from 2.7 to 2.9 Å, perfectly in line with the expected values. In thrombin–TBA–Na, the sodium ion is too small to bind simultaneously the eight oxygens and two alternative positions of Na^+ with the same occupancy were refined according to the electron density. In each position, the ion is closer to four oxygen atoms not lying on the same quartet plane, with distances ranging between 2.2 and 2.7 Å. Ions are also known to play a role in the stabilization of the aptamer loops and may affect the whole quadruplex fold by discriminating among different loop conformations (49). For this reason, particular attention was devoted to verify the presence of ions bound to these TBA regions. The visual inspection of the anomalous map (Supplementary Figure S1) clearly shows that the only potassium ion bound to TBA is the one sandwiched between the two tetrads. Moreover, the electron density of the sodium structure, as well as that of the potassium structure, also gives no evidence for the presence of sodium ions bound to loops. Therefore, the small structural differences between the two complexes must be uniquely related to the type of ion bound in the central core of the aptamer.

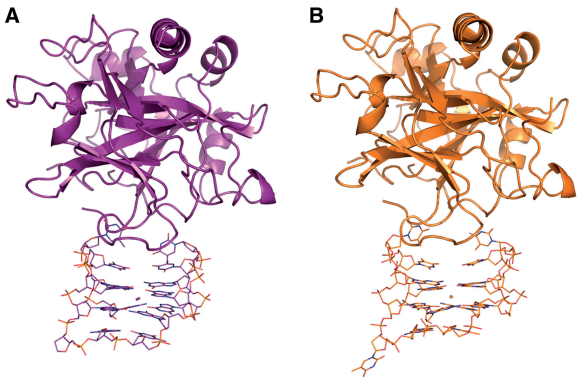

Figure 3. Overall structure of the thrombin–TBA complex in the presence of sodium (**A**) and potassium (**B**) ions. Thrombin molecule is represented as cartoon, TBA molecule is represented as sticks.

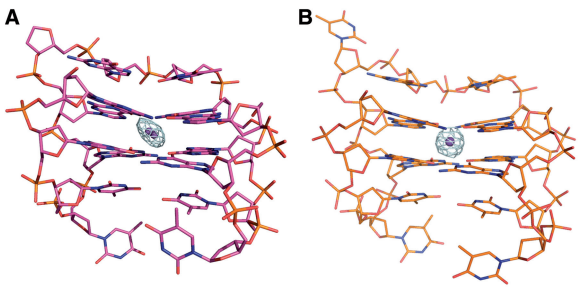

Figure 4. Omit Fo–Fc electron density map (6.0 σ level) of the ion stacked between aptamer quartets in the thrombin–TBA–Na (**A**) and thrombin–TBA–K (**B**) structures.

Architecture of the complex: comparison with previous structures

The crystallographic structures of the complex between α-thrombin and TBA definitely show that the aptamer interacts with the fibrinogen binding site of thrombin by TT loops, as previously found for the modified aptamer mTBA (39). However, the binding mode on thrombin observed for TBA in the present structures differs by a 180° rotation about the helix axis when compared with thrombin–mTBA (PDB code 3QLP) and also with the old thrombin–TBA (PDB code 1HAO) structures (Figure 5). It should be stressed that, apart from the TGT loop, TBA has an approximate 2-fold symmetry coincident with the helix axis. Therefore, as the TGT loop is far away from the protein-binding site, the two binding modes are practically equivalent and can only be distinguished by observing the electron density corresponding to the TGT loop (Figure 5A and B). On the other hand, the packing interactions involving the TGT loop would be different for the two binding modes.

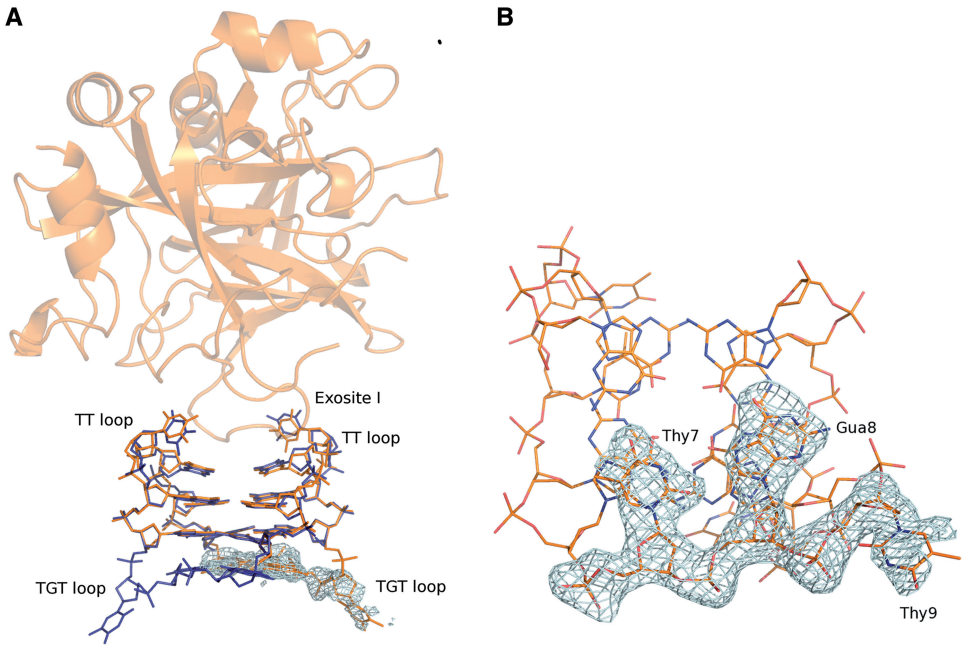

Figure 5. (**A**) Comparison between the two alternative binding modes of TBA: the one observed in the present structures (aptamer is colored in orange) and the one observed in thrombin–mTBA and 1HAO structures (aptamer is colored blue). Omit Fo–Fc electron density map (3σ level) of the TGT loop is also shown. (**B**) Zoomed vision of the TGT loop with its omit Fo–Fc electron density map (3σ level).

TBA in its interactions with α-thrombin

As previously found for the thrombin–mTBA complex (39), the interactions between TBA and α-thrombin are both hydrophobic and hydrophilic and involve residues of the TT loops with a further contribution of Gua5. Thy4 and Thy13 are mainly involved in polar interactions (Supplementary Figure S2), whereas Thy3 and Thy12 form essentially hydrophobic contacts. Several protein residues, such as Arg75, Tyr76, Arg77A and Ile79, are involved in the binding of both aptamers (Table 1), whereas few other residues bind specifically either TBA (His71 and Tyr117) or mTBA (Leu65 and Ile82). Moreover, due to the good quality of the electron density maps, several networks of water molecules bridging thrombin and TBA have been identified; they involve Thr74, Gly69, Ser27 and Lys70 (Table S3).

Focusing the attention on the thrombin/TBA interactions in the Na^+ and K^+ complexes, it emerges that the Na^+ complex is characterized by a slightly larger buried surface area (502 versus 445 $Å^2$), higher surface complementarity index Sc (0.76 vs. 0.72), higher number of interface residues and intermolecular interactions (Table 1), which are the result of correlated small re-arrangements at the exosite I of thrombin and at the TT loops of TBA. In particular, His71 in thrombin–TBA–K adopts two alternative conformations: both conformations are characterized by hydrophobic contacts between the imidazol group and Thy3, and one of them is further stabilized by a polar interaction between ND1 of the histidine and O4 of thymine. These contacts are missing in thrombin–TBA–Na; here, Thy3 is slightly more distant from His71, which adopts a unique conformation (Figure 6A and B).

Placed on the opposite site of the TT loops with respect to the central tetrads, the TGT loop is not involved in thrombin binding and only marginally participates to packing contacts. Thy7 and Gua8 have a similar conformation in the presence of either Na^+ or K^+. The orientation of these residues is fixed by stacking interactions with the tetrad formed by Gua1, Gua6, Gua10, Gua15 and by the binding with a water molecule bridging the N3 atom of Thy7, the N7 atom of Gua8 and the O6 atoms of Gua6 and Gua10. On the other hand, the third base of the loop, Thy9, is not involved in specific interactions and its position is less well defined. Moreover, in the case of thrombin–TBA–Na complex, its mobility is further enhanced by the generally more elevated values of thermal displacement parameters of this structure with respect to that of the potassium complex, and its density is barely visible.

DISCUSSION

Aptamer molecules that are able to recognize and bind human α-thrombin with affinity ranging from low picomolar to low nanomolar represent an attractive approach in the cardiovascular therapy. In general, the high affinity of aptamers derives from contact complementarity between functional groups; their three-dimensional arrangement assures specificity and allows discrimination of the target and non-target homologous proteins (50). Thus, knowledge of the structural details of the interaction between these molecules and their target proteins is crucial for the improvement of aptamers properties.

Although TBA was the first aptamer to be discovered (4) and is still one of the most studied, a detailed picture of

Table 1. Interactions between thrombin and aptamers

	Thrombin–TBA–K (4DII)		Thrombin–TBA–Na (4DIH)		Thrombin–TBA (1HAO)		Thrombin–mTBA (3QLP)	
	Aptamer residue	Protein residue	Aptamer residue	Protein residue	Aptamer residue	Protein residue	Aptamer residue	Protein residue
Polar	Thy3 (O4)	His71 (ND1)	Thy3 (N3)	Glu77 (OE2)	–	–	Thy12 (N3)	Glu77 (OE2)
Polar	Thy4 (O4)	Arg75 (NH2)	Thy4 (O4)	Arg75 (NH1, NH2)	–	–	Thy13 (O4)	Arg75 (NH1, NH2)
Polar	Thy4 (O2)	Arg77A (NH1)	Thy4 (O2)	Arg77A (NH1)	–	–	Thy13 (O3′)	Asn78 (ND2)
Polar	Thy4 (N1)	Arg77A (O)	Thy4 (N1, N3)	Arg77A (O)	–	–	–	–
Polar	Gua5 (O4′)	Arg77A (NH2)	Gua5 (O4′)	Arg77A (NH2)	–	–	Gua2 (O2P)	Arg77A (NH1, NH2)
Polar	Thy13 (O2)	Arg75 (NE, NH2)	Thy13 (O2)	Arg75 (NH2)	–	–	Thy4 (O2)	Arg75 (NH2)
Polar	Thy13 (O4′)	Tyr76 (N)	Thy13 (O4′)	Tyr76 (N)	–	–	Thy4 (O4′)	Tyr76 (N)
Polar	Thy13 (N3)	Tyr76 (O)	Thy13 (N3)	Tyr76 (O)	–	–	Thy4 (O4)	Arg77A (NH1)
Hydrophobic	Thy3	His71, Ile79, Tyr117	Thy3	Ile24, Ile79, Tyr117	Thy12	Ile24, His71, Ile79, Tyr117	Thy12	Ile79
Hydrophobic	Thy4	Asn78, Ile79	Thy4	Ile79	–	–	Thy13	Asn78, Ile79
Hydrophobic	Thy12	–	Thy12	Tyr76	Thy3	Tyr76, Ile82	Thy3	Tyr76, Leu65, Ile82
Hydrophobic	Thy13	Tyr76	Thy13	Tyr76	–	–	Thy4	Tyr76

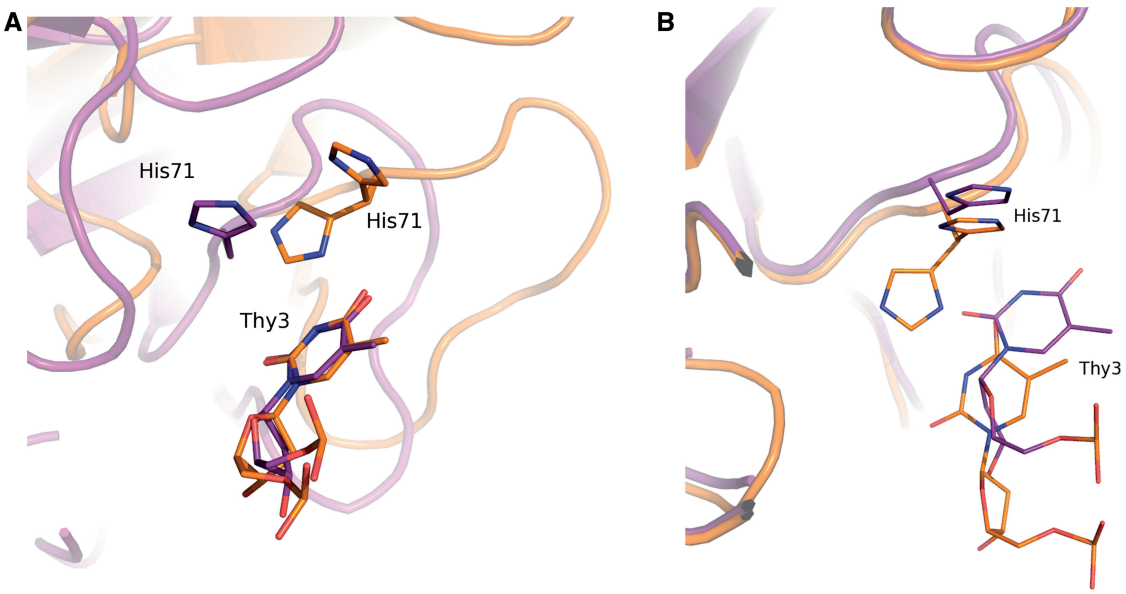

Figure 6. Different position of His71 with respect to Thy3 in thrombin–TBA–Na (purple) and thrombin–TBA–K (orange) upon superposition of (**A**) Thy3 and (**B**) protein backbone atoms.

its complex with human α-thrombin has not yet been fully clarified. The recently published structure of thrombin in complex with mTBA at 2.15 Å resolution has provided new structural information on the thrombin–aptamers recognition process (39); those results are now fully confirmed by the high-resolution structures of thrombin–TBA complex crystallized in the presence of the monovalent cations K^+ or Na^+. In particular, the proposed 1:1 stoichiometry of the complex in solution relies on the 1:1 stoichiometry present in all crystal forms and on the extended interaction surface between the exosite I of the thrombin and the TT loops of aptamers that remains essentially unmodified in all crystal forms. On the other side, the TGT loop is involved in non specific packing contacts that change from one crystal form to the other. Thus, the present structures strongly enforce the previous suggestion (39) that the TT loops, acting as a pincer-like system that embraces the protruding region of thrombin exosite I, are the aptamer binding motif. It is noteworthy to recall that in the two crystal structures here presented the aptamer is rotated 180° about its pseudo 2-fold axis with respect to thrombin–mTBA and 1HAO structures.

As far as the complex with TBA is concerned, the two binding modes are basically equivalent and the only significant difference is confined to the orientation of the TGT loop that is far away from the binding contacts with α-thrombin. On the other hand, for the putative 1:1 complex in solution the TGT loop is expected to be fully exposed to the solvent. Therefore, it can be supposed that both binding modes involving TT loops exist in solution and just one of them is selected in the crystallization process. The deviations from the 2-fold symmetry are much larger for mTBA due to the polarity inversion site. Thus, the interactions with the protein for the two binding modes are not fully equivalent and it can be expected that also in solution only one species is significantly populated. These features are in line with the thermodynamic data, indicating a less adverse entropic contribute for the formation of the complex between thrombin and TBA with respect to mTBA (12).

The differences in the functional properties of TBA and mTBA have been previously analysed on the basis of the crystal structures of the thrombin–mTBA complex and 1HAO model. Interestingly, the surface complementarity indexes obtained for thrombin–TBA–K and thrombin–TBA–Na are much higher than that calculated for the old 1HAO model and almost comparable with that of thrombin–mTBA. However, the buried surface areas are in both cases smaller than the one found for the modified aptamer. These findings confirm the previous suggestion that the greater affinity for α-thrombin of mTBA with respect to TBA is related to a better fit of mTBA at the thrombin exosite I and to a larger buried area (39). The greater number of contacts between mTBA and α-thrombin when compared with TBA does agree with the larger favourable enthalpy in the complex formation (12).

The effects of the alkaline ion on the properties of the thrombin–TBA complex are particularly interesting. CD shows that both ions stabilize the typical anti-parallel G-quadruplex structure of TBA, and this conformation is further stabilized by the binding with α-thrombin. As well known (51,52), the effect of K^+ is much greater than that of Na^+, as proved also by the T_m values in the presence and in the absence of α-thrombin. The analysis of the aptamer atomic thermal displacement parameters relative to those of thrombin molecule see definition in ref. (53) indicates a greater flexibility of TBA–Na with respect to the K^+ counterpart. Indeed, the potassium ion perfectly fits at the center of the cavity between the two G-tetrads and links together all the eight purine O6 atoms in a distorted anti-prism geometry at the expected coordination distances, thus increasing the rigidity and the stability of the whole structure. Because of its smaller size, the sodium ion is partially disordered and occupies two alternative positions, each one closer to one of the two tetrads. This confers a higher plasticity to the aptamer that favours a better fit on the thrombin surface and the optimization of the intermolecular contacts, as evidenced by the data regarding the buried surface area. In the absence of thrombin, K^+ markedly stabilizes TBA when compared with the Na^+ containing aptamer (T_m = 53 and 24°C in the case of TBA–K and TBA–Na, respectively). The stability of the ternary complexes with thrombin is considerably higher, but the relative effect of the two ions is reduced (70 and 58°C for thrombin–TBA–K and thrombin–TBA–Na, respectively), in agreement with the more extended aptamer/thrombin contacts in the Na^+ vs. K^+ ternary complexes. However, in the presence of sodium ions, the binding of the protein does not reduce the local flexibility of the aptamer core, caused by the smaller ionic radius of Na^+ with respect to K^+. Thus, thrombin–TBA–Na stability is still lower than that of thrombin–TBA–K.

The present results are of particular interest as they underline the subtle effects of the specific binding site and type of the ionic species in the modulation of the protein/aptamer recognition. Incidentally, an alternative localization of the alkaline ion between quartets and loops was hypothesized in the past (54–56). Very recently, the correct positioning of the ion in between the two tetrads has been suggested on the basis of molecular dynamics simulation (57,58) and NMR studies in the presence of NH_4^+ as counter ion (59). The present structures represent the first detailed description of the ionic binding site of TBA.

The alkaline ions also influence the inhibitory activity of TBA, which is lower in the presence of Na^+ with respect to K^+. In the conditions used for the assays, TBA is folded and its complex with thrombin is stable in the presence of Na^+ as well as of K^+. Therefore, the different effects on the inhibitory activity of TBA should arise from some subtle structural differences of the corresponding complexes. Indeed, we have found that in thrombin–TBA–K the aptamer interacts with His71, a residue crucial for the inhibition of the fibrinogen conversion to fibrin by α-thrombin. Contacts with this thrombin residue are missing in the case of thrombin–TBA–Na; thus, His71 remains more free to interact with fibrinogen and this may explain the lower inhibitory activity of the thrombin/TBA adduct in the presence of Na^+.

The interplay between affinity of the ion and flexibility induced by its binding to the thrombin/aptamer adduct plays an intriguing role in determining the relevance of the inhibition process and deserves a special attention in the design of new aptamers aimed to an enhanced activity.

ACCESSION NUMBERS

PDB CODES: 4DIH and 4DII.

SUPPLEMENTARY DATA

Supplementary Data are available at NAR Online: Supplementary Tables 1–3 and Supplementary Figures 1 and 2.

ACKNOWLEDGEMENTS

We acknowledge Giosuè Sorrentino and Maurizio Amendola (Institute of Biostructures and Bioimages, Naples, Italy) for technical assistance.

FUNDING

Funding for open access charge: Italian Institute of Technology (IIT); Italian M.U.R.S.T. (P.R.I.N. 2009).

Conflict of interest statement. None declared.

REFERENCES

1. Gellert,M., Lipsett,M.N. and Davies,D.R. (1962) Helix formation by guanylic acid. *Proc. Natl. Acad. Sci. USA*, **48**, 2013–2018.
2. Williamson,J.R. (1994) G-quartet structures in telomeric DNA. *Annu. Rev. Biophys. Biomol. Struct.*, **23**, 703–730.
3. Burge,S., Parkinson,G.N., Hazel,P., Todd,A.K. and Neidle,S. (2006) Quadruplex DNA: sequence, topology and structure. *Nucleic Acids Res.*, **34**, 5402–5415.
4. Bock,L.C., Griffin,L.C., Latham,J.A., Vermaas,E.H. and Toole,J.J. (1992) Selection of single-stranded DNA molecules that bind and inhibit human thrombin. *Nature*, **355**, 564–566.
5. Burke,J.M. and Berzal-Herranz,A. (1993) *In vitro* selection and evolution of RNA: applications for catalytic RNA, molecular recognition, and drug discovery. *FASEB J.*, **7**, 106–112.
6. Huntington,J.A. (2005) Molecular recognition mechanisms of thrombin. *J. Thromb. Haemost.*, **3**, 1861–1872.
7. Macaya,R.F., Schultze,P., Smith,F.W., Roe,J.A. and Feigon,J. (1993) Thrombin-binding DNA aptamer forms a unimolecular quadruplex structure in solution. *Proc. Natl. Acad. Sci. USA*, **90**, 3745–3749.
8. Wang,K.Y., McCurdy,S., Shea,R.G., Swaminathan,S. and Bolton,P.H. (1993) A DNA aptamer which binds to and inhibits thrombin exhibits a new structural motif for DNA. *Biochemistry*, **32**, 1899–1904.
9. Mao,X., Marky,L.A. and Gmeiner,W.H. (2004) NMR structure of the thrombin-binding DNA aptamer stabilized by Sr^{2+}. *J. Biomol. Struct. Dyn.*, **22**, 25–33.
10. Martino,L., Virno,A., Randazzo,A., Virgilio,A., Esposito,V., Giancola,C., Bucci,M., Cirino,G. and Mayol,L. (2006) A new modified thrombin binding aptamer containing a 5′-5′ inversion of polarity site. *Nucleic Acids Res.*, **34**, 6653–6662.
11. Nallagatla,S.R., Heuberger,B., Haque,A. and Switzer,C. (2009) Combinatorial synthesis of thrombin-binding aptamers containing iso-guanine. *J. Comb. Chem.*, **11**, 364–369.
12. Pagano,B., Martino,L., Randazzo,A. and Giancola,C. (2008) Stability and binding properties of a modified thrombin binding aptamer. *Biophys. J.*, **94**, 562–569.
13. Nagatoishi,S., Isono,N., Tsumoto,K. and Sugimoto,N. (2011) Loop residues of thrombin-binding DNA aptamer impact G-quadruplex stability and thrombin binding. *Biochimie*, **93**, 1231–1238.
14. Pasternak,A., Hernandez,F.J., Rasmussen,L.M., Vester,B. and Wengel,J. (2011) Improved thrombin binding aptamer by incorporation of a single unlocked nucleic acid monomer. *Nucleic Acids Res.*, **39**, 1155–1164.
15. Zaitseva,M., Kaluzhny,D., Shchyolkina,A., Borisova,O., Smirnov,I. and Pozmogova,G. (2010) Conformation and thermostability of oligonucleotide d(GGTTGGTGTGGTTGG) containing thiophosphoryl internucleotide bonds at different positions. *Biophys. Chem.*, **146**, 1–6.
16. Saneyoshi,H., Mazzini,S., Avino,A., Portella,G., Gonzalez,C., Orozco,M., Marquez,V.E. and Eritja,R. (2009) Conformationally rigid nucleoside probes help understand the role of sugar pucker and nucleobase orientation in the thrombin-binding aptamer. *Nucleic Acids Res.*, **37**, 5589–5601.
17. Bonifacio,L., Church,F.C. and Jarstfer,M.B. (2008) Effect of locked-nucleic acid on a biologically active G-quadruplex. A structure-activity relationship of the thrombin aptamer. *Int. J. Mol. Sci.*, **9**, 422–433.
18. Virno,A., Randazzo,A., Giancola,C., Bucci,M., Cirino,G. and Mayol,L. (2007) A novel thrombin binding aptamer containing a G-LNA residue. *Bioorg. Med. Chem.*, **15**, 5710–5718.
19. Kankia,B.I. and Marky,L.A. (2001) Folding of the thrombin aptamer into a G-quadruplex with Sr(2+): stability, heat, and hydration. *J. Am. Chem. Soc.*, **123**, 10799–10804.
20. Mao,X.A. and Gmeiner,W.H. (2005) NMR study of the folding-unfolding mechanism for the thrombin-binding DNA aptamer d(GGTTGGTGTGGTTGG). *Biophys. Chem.*, **113**, 155–160.
21. Mayer,G., Muller,J., Mack,T., Freitag,D.F., Hover,T., Potzsch,B. and Heckel,A. (2009) Differential regulation of protein subdomain activity with caged bivalent ligands. *ChemBioChem*, **10**, 654–657.
22. Smirnov,I. and Shafer,R.H. (2000) Effect of loop sequence and size on DNA aptamer stability. *Biochemistry*, **39**, 1462–1468.
23. Tang,C.F. and Shafer,R.H. (2006) Engineering the quadruplex fold: nucleoside conformation determines both folding topology and molecularity in guanine quadruplexes. *J. Am. Chem. Soc.*, **128**, 5966–5973.
24. Smirnov,I. and Shafer,R.H. (2000) Lead is unusually effective in sequence-specific folding of DNA. *J. Mol. Biol.*, **296**, 1–5.
25. Marathias,V.M., Wang,K.Y., Kumar,S., Pham,T.Q., Swaminathan,S. and Bolton,P.H. (1996) Determination of the number and location of the manganese binding sites of DNA quadruplexes in solution by EPR and NMR in the presence and absence of thrombin. *J. Mol. Biol.*, **260**, 378–394.
26. Nimjee,S.M., Rusconi,C.P., Harrington,R.A. and Sullenger,B.A. (2005) The potential of aptamers as anticoagulants. *Trends Cardiovasc. Med.*, **15**, 41–45.
27. Griffin,L.C., Tidmarsh,G.F., Bock,L.C., Toole,J.J. and Leung,L.L. (1993) *In vivo* anticoagulant properties of a novel nucleotide-based thrombin inhibitor and demonstration of regional anticoagulation in extracorporeal circuits. *Blood*, **81**, 3271–3276.
28. Li,W.X., Kaplan,A.V., Grant,G.W., Toole,J.J. and Leung,L.L. (1994) A novel nucleotide-based thrombin inhibitor inhibits clot-bound thrombin and reduces arterial platelet thrombus formation. *Blood*, **83**, 677–682.
29. Gatto,B., Palumbo,M. and Sissi,C. (2009) Nucleic acid aptamers based on the G-quadruplex structure: therapeutic and diagnostic potential. *Curr. Med. Chem.*, **16**, 1248–1265.
30. Tennico,Y.H., Hutanu,D., Koesdjojo,M.T., Bartel,C.M. and Remcho,V.T. (2010) On-chip aptamer-based sandwich assay for thrombin detection employing magnetic beads and quantum dots. *Anal. Chem.*, **82**, 5591–5597.
31. Liang,G., Cai,S., Zhang,P., Peng,Y., Chen,H., Zhang,S. and Kong,J. (2011) Magnetic relaxation switch and colorimetric detection of thrombin using aptamer-functionalized gold-coated iron oxide nanoparticles. *Anal. Chim. Acta*, **689**, 243–249.
32. Platt,M., Rowe,W., Wedge,D.C., Kell,D.B., Knowles,J. and Day,P.J. (2009) Aptamer evolution for array-based diagnostics. *Anal. Biochem.*, **390**, 203–205.
33. Padmanabhan,K., Padmanabhan,K.P., Ferrara,J.D., Sadler,J.E. and Tulinsky,A. (1993) The structure of alpha-thrombin inhibited by a 15-mer single-stranded DNA aptamer. *J. Biol. Chem.*, **268**, 17651–17654.
34. Padmanabhan,K. and Tulinsky,A. (1996) An ambiguous structure of a DNA 15-mer thrombin complex. *Acta Crystallogr. D Biol. Crystallogr.*, **52**, 272–282.
35. Kelly,J.A., Feigon,J. and Yeates,T.O. (1996) Reconciliation of the X-ray and NMR structures of the thrombin-binding aptamer d(G GTTGGTGTGGTTGG). *J. Mol. Biol.*, **256**, 417–422.
36. Tsiang,M., Gibbs,C.S., Griffin,L.C., Dunn,K.E. and Leung,L.L. (1995) Selection of a suppressor mutation that restores affinity of an oligonucleotide inhibitor for thrombin using in vitro genetics. *J. Biol. Chem.*, **270**, 19370–19376.
37. Tasset,D.M., Kubik,M.F. and Steiner,W. (1997) Oligonucleotide inhibitors of human thrombin that bind distinct epitopes. *J. Mol. Biol.*, **272**, 688–698.
38. Baldrich,E. and O'Sullivan,C.K. (2005) Ability of thrombin to act as molecular chaperone, inducing formation of quadruplex structure of thrombin-binding aptamer. *Anal. Biochem.*, **341**, 194–197.
39. Russo Krauss,I., Merlino,A., Giancola,C., Randazzo,A., Mazzarella,L. and Sica,F. (2011) Thrombin-aptamer recognition: a revealed ambiguity. *Nucleic Acids Res.*, **39**, 7858–7867.
40. Russo Krauss,I., Merlino,A., Randazzo,A., Mazzarella,L. and Sica,F. (2010) Crystallization and preliminary X-ray analysis of the complex of human alpha-thrombin with a modified

thrombin-binding aptamer. *Acta Crystallogr. Sect. F Struct. Biol. Cryst. Commun.*, **66**, 961–963.
41. Otwinowsky,Z. and Minor,W. (1997) Processing of X-ray diffraction data collected in oscillation mode. *Methods Enzymol.*, **276**, 307–326.
42. McCoy,A.J., Grosse-Kunstleve,R.W., Storoni,L.C. and Read,R.J. (2005) Likelihood-enhanced fast translation functions. *Acta Crystallogr. D Biol. Crystallogr.*, **61**, 458–464.
43. Brunger,A.T., Adams,P.D., Clore,G.M., DeLano,W.L., Gros,P., Grosse-Kunstleve,R.W., Jiang,J.S., Kuszewski,J., Nilges,M., Pannu,N.S. *et al.* (1998) Crystallography & NMR system: a new software suite for macromolecular structure determination. *Acta Crystallogr. D Biol. Crystallogr.*, **54(Pt 5)**, 905–921.
44. Jones,T.A., Zou,J.Y., Cowan,S.W. and Kjeldgaard,M. (1991) Improved methods for building protein models in electron density maps and the location of errors in these models. *Acta Crystallogr. A*, **47(Pt 2)**, 110–119.
45. Collaborative Computational Project. (1994) The CCP4 suite: programs for protein crystallography. *Acta Crystallogr. D Biol. Crystallogr.*, **50**, 760–763.
46. Laskowski,R.A., MacArthur,M.W., Moss,M.D. and Thorton,J.M. (1993) PROCHECK: a program to check the stereochemical quality of protein structure. *J. Appl. Crystallogr.*, **26**, 283–291.
47. Hooft,R.W., Vriend,G., Sander,C. and Abola,E.E. (1996) Errors in protein structures. *Nature*, **381**, 272.
48. Lawrence,M.C. and Colman,P.M. (1993) Shape complementarity at protein/protein interfaces. *J. Mol. Biol.*, **234**, 946–950.
49. Wei,D., Parkinson,G., Reszka,A.P. and Neidle,S. (2012) Crystal structure of a c-kit promoter quadruplex reveals the structural role of metal ions and water molecules in maintaining loop conformation. *Nucleic Acids Res.*, **40**, 4691–4700.
50. Becker,R.C., Povsic,T., Cohen,M.G., Rusconi,C.P. and Sullenger,B. (2010) Nucleic acid aptamers as antithrombotic agents: opportunities in extracellular therapeutics. *Thromb. Haemost.*, **103**, 586–595.
51. Hud,N.V., Smith,F.W., Anet,F.A. and Feigon,J. (1996) The selectivity for K^+ versus Na^+ in DNA quadruplexes is dominated by relative free energies of hydration: a thermodynamic analysis by 1H NMR. *Biochemistry*, **35**, 15383–15390.
52. Lane,A.N., Chaires,J.B., Gray,R.D. and Trent,J.O. (2008) Stability and kinetics of G-quadruplex structures. *Nucleic Acids Res.*, **36**, 5482–5515.
53. Kim,S.Y., Hwang,K.Y., Kim,S.H., Sung,H.C., Han,Y.S. and Cho,Y. (1999) Structural basis for cold adaptation. Sequence, biochemical properties, and crystal structure of malate dehydrogenase from a psychrophile *Aquaspirillium arcticum*. *J. Biol. Chem.*, **274**, 11761–11767.
54. Hong,E.S., Yoon,H.J., Kim,B., Yim,Y.H., So,H.Y. and Shin,S.K. (2010) Mass spectrometric studies of alkali metal ion binding on thrombin-binding aptamer DNA. *J. Am. Soc. Mass Spectrom.*, **21**, 1245–1255.
55. Marathias,V.M. and Bolton,P.H. (1999) Determinants of DNA quadruplex structural type: sequence and potassium binding. *Biochemistry*, **38**, 4355–4364.
56. Marathias,V.M. and Bolton,P.H. (2000) Structures of the potassium-saturated, 2:1, and intermediate, 1:1, forms of a quadruplex DNA. *Nucleic Acids Res.*, **28**, 1969–1977.
57. Reshetnikov,R.V., Golovin,A.V., Spiridonova,V., Kopylov,A.M. and Sponer,J. (2010) Structural dynamics of thrombin-binding DNA aptamer d(GGTTGGTGTGGTTGG) quadruplex DNA studied by large-scale explicit solvent simulations. *J. Chem. Theory Comput.*, **6**, 3003–3014.
58. Reshetnikov,R.V., Sponer,J., Rassokhina,O.I., Kopylov,A.M., Tsvetkov,P.O., Makarov,A.A. and Golovin,A.V. (2011) Cation binding to 15-TBA quadruplex DNA is a multiple-pathway cation-dependent process. *Nucleic Acids Res.*, **39**, 9789–9802.
59. Trajkovski,M., Sket,P. and Plavec,J. (2009) Cation localization and movement within DNA thrombin binding aptamer in solution. *Org. Biomol. Chem.*, **7**, 4677–4684.